Available online at www.sciencedirect.com
ScienceDirect
Cement & Concrete Composites 28 (2006) 949–958
Cement & Concrete Composites
www.elsevier.com/locate/cemconcomp

FRP-confined concrete under axial cyclic compression

L. Lam [a], J.G. Teng [a,*], C.H. Cheung [a], Y. Xiao [b]

[a] Department of Civil and Structural Engineering, Hong Kong Polytechnic University, Hung Hom, Hong Kong, Kowkoon, China
[b] Department of Civil Engineering, School of Engineering, University of Southern California, Los Angeles, California, USA

Available online 7 September 2006

Abstract

One important application of fiber reinforced polymer (FRP) composites in construction is as FRP jackets to confine concrete in the seismic retrofit of reinforced concrete (RC) structures, as FRP confinement can enhance both the compressive strength and ultimate strain of concrete. For the safe and economic design of FRP jackets, the stress–strain behavior of FRP-confined concrete under cyclic compression needs to be properly understood and modeled. This paper presents the results of an experimental study on the behavior of FRP-confined concrete under cyclic compression. Test results obtained from CFRP-wrapped concrete cylinders are presented and examined, which allows a number of significant conclusions to be drawn, including the existence of an envelope curve and the cumulative effect of loading cycles. The results are also compared with two existing stress–strain models for FRP-confined concrete, one for monotonic loading and another one for cyclic loading. The monotonic stress–strain model of Lam and Teng is shown to be able to provide accurate predictions of the envelope curve, but the only existing cyclic stress–strain model is shown to require improvement.

Keywords: FRP; Confinement; Concrete; Cyclic loading; Stress–strain models

1. Introduction

Fiber reinforced polymer (FRP) composites have found increasingly wide applications in civil engineering due to their high strength-to-weight ratio and high corrosion resistance. One important application of FRP-composites is as a confining material for concrete, in both the retrofit of existing reinforced concrete (RC) columns and in concrete-filled FRP tubes in new construction [1–3]. As a result of FRP confinement, both the compressive strength and the ultimate strain of concrete can be greatly enhanced. In both types of applications, the stress–strain behavior of FRP-confined concrete, under both monotonic and cyclic compression, needs to be properly understood and modeled. The stress–strain behavior of confined concrete under cyclic compression is of particular interest in the seismic retrofit and design of concrete structures.

Many studies have examined the stress–strain behavior of unconfined and steel-confined concrete under cyclic compression (e.g. [4–12]). In the past decade, extensive research has also been conducted on the monotonic stress–strain behavior of FRP-confined concrete (e.g. [13–25]), but only a few studies have been concerned with FRP-confined concrete under cyclic compression [26–33]. While the latter studies provided limited but valuable experimental results, considerable uncertainties still exist in several issues, including the ultimate condition of FRP-confined concrete under cyclic compression in comparison with the case of monotonic compression [34], the effect of loading history on the stress–strain response, and the accurate modeling of the stress–strain behavior. To the best knowledge of the authors, only one cyclic stress–strain model has been proposed for FRP-confined concrete by Shao [33] based mainly on his own limited test data.

This paper presents the results of a recent experimental study on the behavior of FRP-confined concrete under cyclic compression. Test results obtained from CFRP-wrapped concrete cylinders are presented and examined

* Corresponding author. Tel.: +852 2766 6012; fax: +852 2334 6389.
E-mail address: cejgteng@polyu.edu.hk (J.G. Teng).

0958-9465/$ - see front matter © 2006 Elsevier Ltd. All rights reserved.
doi:10.1016/j.cemconcomp.2006.07.007

first. These results are then compared with two existing models for FRP-confined concrete, one for monotonic loading and another one for cyclic loading.

2. Experimental details

2.1. Test specimens

A total of 18 concrete cylinders of 152 mm in diameter and 305 mm in height were prepared and tested in two series. Each series consisted of six cylinders confined by carbon FRP (CFRP) jackets, plus three unconfined cylinders as control specimens, all prepared from the same batch of concrete. The CFRP jackets were formed in a wet lay-up process by wrapping a continuous carbon fiber sheet with the impregnation of epoxy resin. The six confined cylinders in Series I were wrapped with one ply of CFRP, and those in Series II were wrapped with two plies of CFRP. An overlap length of 150 mm was included for all wrapped specimens to form a vertical joint. Both the upper and lower ends of each wrapped cylinder were strengthened with an additional CFRP strip of 25 mm in width. These strengthening strips contained one ply of CFRP for the one-ply jackets and two plies of CFRP for the two-ply jackets. Table 1 provides the key information of the test specimens.

2.2. Strain gauge layout

The axial strains were determined using two linear variable displacement transducers (LVDTs), at 180° apart and covering the mid-height region of 120 mm (Fig. 1(a)). The hoop strains of the concrete cylinders were measured using strain gauges. For each unconfined concrete cylinder, two strain gauges with a gauge length of 60 mm were bonded, at 180° apart, at the mid-height of the cylinder. For each FRP-wrapped concrete cylinder, eight strain gauges with a gauge length of 20 mm were installed at

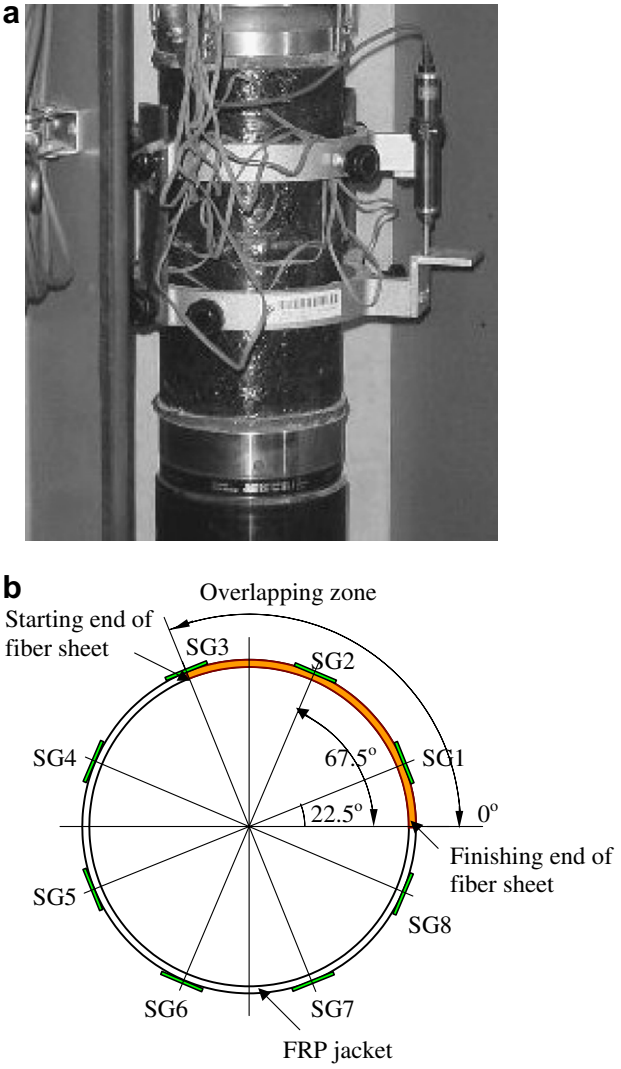

Fig. 1. Test specimen (a) test setup and (b) location of strain gauges for hoop strains in an FRP jacket.

Table 1
Details of CFRP-confined specimens and key test results

Series	Loading pattern	Specimen	f'_{cc} (MPa)	ε_{cu}	$\varepsilon_{h,rup}$	
					Average	Maximum
I	Monotonic	CI-M1	52.6	0.0090	0.0081	0.0088
		CI-M2	57.0	0.0121	0.0108	0.0117
		CI-M3	55.4	0.0111	0.0107	0.0116
	Single cycles at prescribed displacements	CI-SC1	60.2	0.0134	0.0132[a]	0.0143[a]
		CI-SC2	56.8	0.0117	0.0103	0.0112
	Three repeated cycles at prescribed displacements	CI-RC	56.5	0.0120	0.0113	0.01224
II	Monotonic	CII-M1	76.8	0.0191	0.0106	0.0120
		CII-M2	79.1	0.0208	0.0113	0.0121
		CII-M3	65.8	0.0125	0.0079	0.0090
	Single cycles at prescribed displacements	CII-SC1	81.5	0.0244	0.0122	0.0131
		CII-SC2	78.2	0.0189	0.0108	0.0120
	Three repeated cycles at prescribed displacements	CII-RC	85.6	0.0234	0.0122	0.0139

[a] One strain gauge outside the overlapping zone was damaged.

the mid-height of the cylinder, which were evenly distributed around the circumference to measure the hoop strains of the FRP jacket. Five of them were located outside the overlapping zone, and the remaining three located in the overlapping zone (Fig. 1(b)). This strain measurement scheme was employed to study the hoop strain distribution in and the ultimate condition of the FRP jacket under cyclic compression. Further details of the strain gauge layout can be found in Ref. [34], which is concerned with the ultimate condition of FRP-confined concrete in monotonic compression.

2.3. Compression tests

The compression tests were performed using a 1600 kn capacity servo-controlled MTS testing machine under displacement control (stroke control) at a constant rate of 0.6 mm/min. It should be noted that this displacement included not only the shortening of the concrete cylinder under compression, but also the deformation of the whole loading system itself.

For the three unconfined cylinders and three of the six FRP-confined cylinders in each series, loading was applied with monotonically increasing displacements until failure. The failure of FRP-confined concrete cylinders was all by the rupture of the FRP jacket. For the other three FRP-confined cylinders in each series, cyclic compression involving unloading and reloading cycles was applied at several unloading displacement values before failure. Two of these three specimens were subjected to a single loading/unloading cycle at each prescribed displacement level. In this case, the specimen was loaded by increasing the axial displacement to a prescribed value, and was next unloaded by reducing the axial displacement to a target load level. The specimen was then reloaded to the next prescribed displacement for cyclic loading. The third FRP-confined cylinder was subjected to three unloading/reloading cycles at each prescribed unloading displacement level. For both cases of cyclic compression, the target load level at which unloading was terminated and reloading started was 20 kn, which is equivalent to an axial stress of about 1.1 MPa. All the loading patterns were automatically executed by a computer program. Readings of the load, displacement, strain gauges and LVDTs were taken using a data logging system and were stored in a computer.

2.4. Properties of CFRP

The wet lay-up CFRP system used in this study included unidirectional carbon fiber sheets and epoxy-based primer and resin. The carbon fiber sheets had a nominal thickness of 0.165 mm. The measured thicknesses of the CFRP outside the overlapping zone were 0.69 mm in one-ply jackets and 1.09 mm in two-ply jackets, respectively. The elastic moduli of the CFRP were 250 GPa for one-ply jackets and 247 GPa for two-ply jackets respectively, which were determined from flat coupon tests according to ASTM D3039 [35] and calculated based on the nominal thickness of the CFRP sheet, accounting for the effect of the actual thickness of the CFRP sheet [34]. The ultimate tensile strain of the CFRP from these flat coupon tests was 1.52%.

3. Test results

The compression tests of the unconfined concrete cylinders showed that the concrete for the Series I specimens

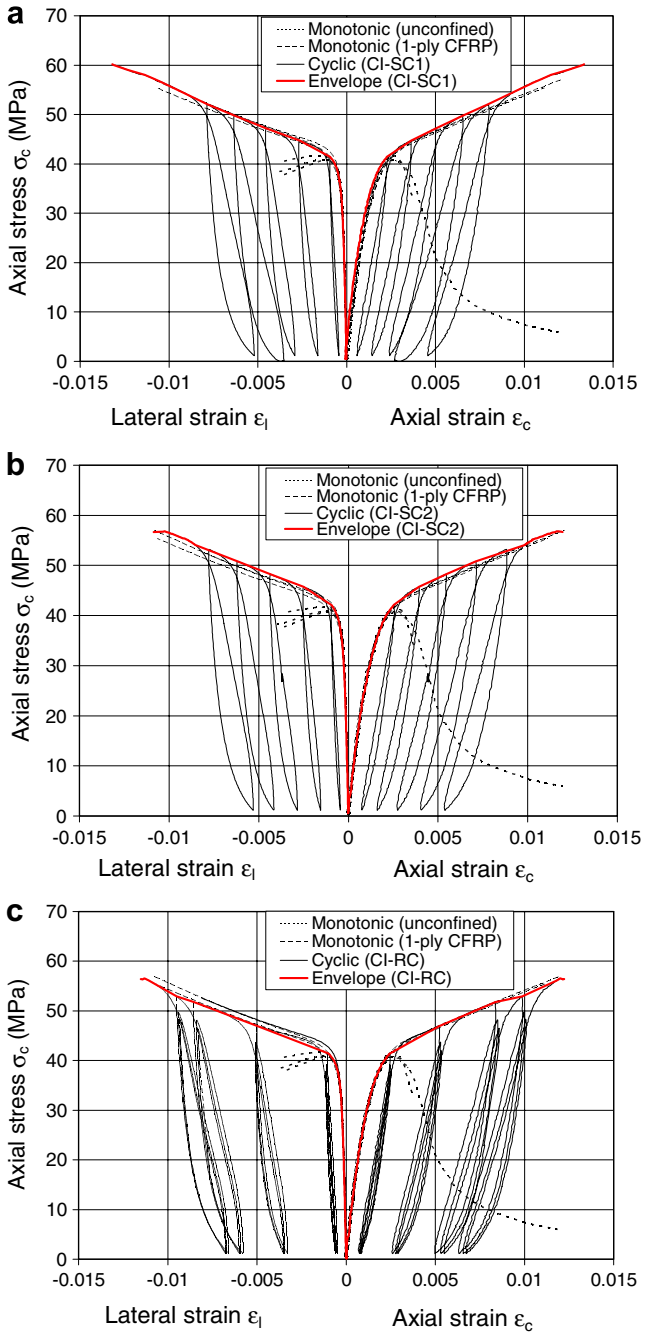

Fig. 2. Cyclic stress–strain curves of concrete confined with one ply of CFRP in comparison with monotonic stress–strain curves of confined and unconfined concrete. (a) Specimen CI-SC1, (b) specimen CI-SC2, and (c) CI-RC.

had an unconfined concrete compressive strength f'_{co} of 41.1 MPa at an axial strain of 0.00256, while the concrete for the Series II specimens had an unconfined concrete strength f'_{co} of 38.9 at an axial strain of 0.0025.

All the FRP-confined specimens failed by the rupture of the FRP jacket. The key results are shown in Table 1. The ultimate axial strains of confined concrete ε_{cu} were averaged from the two LVDTs. For the FRP hoop rupture strain $\varepsilon_{h,rup}$, both the average values from strain gauges outside the overlapping zone and the maximum values around the circumference, which also occurred outside the overlapping zone, are presented. Stress–strain curves of FRP-confined concrete under cyclic compression are shown in Fig. 2 for specimens confined with one ply of CFRP, and in Fig. 3 for specimens confined with two plies of CFRP. In each figure, stress–strain curves of three confined and three unconfined concrete specimens under monotonic loading from the same series are also shown for comparison. In plotting these figures, the axial strains ε_c (compressive strains) in concrete are defined as positive, while the lateral strains ε_l are defined as negative and assumed to have the same magnitude as the FRP hoop strains ε_h, which are defined as positive and averaged from the five strain gauges outside the overlapping zone. The strain gauge values within the overlapping zone are affected by the additional thickness due to the overlapping, so the use of the strain values outside the overlapping zone alone provides a more accurate picture of the dilation response of the confined concrete [34]. The critical points include the starting points of unloading and reloading, the reference strain point on the reloading curve, and the estimated zero stress point for the unloading curve. The reference strain is taken as the axial strain at which the first unloading/reloading cycle starts at a prescribed displacement value.

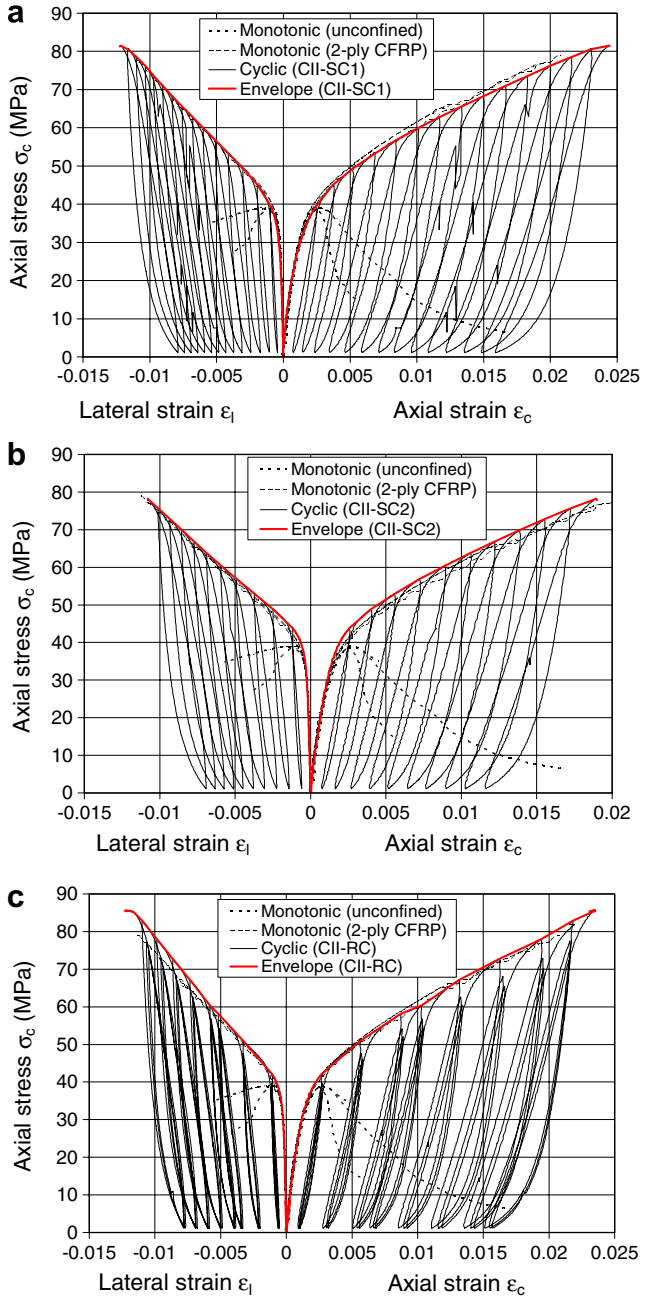

Fig. 3. Cyclic stress–strain curves of concrete confined with two plies of CFRP in comparison with monotonic stress–strain curves of confined and unconfined concrete. (a) Specimen CII-SC1, (b) specimen CII-SC2, and (c) specimen CII-RC.

4. Discussions

4.1. Envelope curve

A basic hypothesis in studies on the cyclic stress–strain behavior of unconfined and steel-confined concrete is that an envelope curve exists and this envelope curve is approximately the same as the stress–strain curve for the same concrete under monotonic loading [5,7]. Such an envelope curve can be considered as the upper boundary of the response of the concrete subjected to different loading histories in the stress–strain domain.

Recently, Rodrigues and Silva [27] suggested the possibility that for FRP-confined concrete, the monotonic stress–strain curve may stay below the envelope curve of the cyclic stress–strain curve, based on their test results of CFRP-confined small RC columns with both longitudinal and transverse steel reinforcement. Other studies by Theodoros [29] and Ilki and Kumbasar [30,31], however, suggested the coincidence of the monotonic curve with the envelope curve of the cyclic curve. An uncertainty in the comparison by Ilki and Kumbasar [30,31] is that the unconfined concrete strengths were slightly different for the specimens under monotonic compression and cyclic compression respectively.

To compare the monotonic and cyclic stress–strain strain curves of FRP-confined concrete, Figs. 2 and 3 show envelope curves for both the axial stress-axial strain and the axial stress–lateral strain curves (heavy solid lines), which were obtained by connecting the initial unloading points on the stress–strain curve within the strain range for cyclic loading. In some of the diagrams shown in these

figures, it is difficult to distinguish the envelope curve from the stress–strain curve from the corresponding monotonic loading test, as the two almost coincide. This observation indicates that the basic hypothesis of envelope curves is valid for FRP-confined concrete. For this reason, the first unloading/reloading cycle at each prescribed axial displacement following monotonic loading can be considered as unloading/reloading from the envelope curve, while the subsequent unloading/reloading cycles are cycles within the envelope curve (i.e., not reaching the envelope curve).

4.2. Plastic strain

The plastic strain of concrete is defined as the residual axial strain of concrete when it is unloaded to the zero stress. In the present study, all the unloading curves except one unloading curve of specimen CI-SC1 were terminated before reaching the zero stress, so the plastic strains had to be estimated by extending the unloading curves to the zero stress. These estimated axial strains at zero stress are shown in Fig. 4.

In a number of existing studies (e.g. [10,12]), the plastic strain of unconfined or steel-confined concrete were related to the axial strain at the starting point of unloading. Sakai and Kawashima [12] suggested that the plastic strain ε_{pl} of steel-confined concrete is a linear function of the unloading strain ε_{un} for each of the two regions of $0.001 \leqslant \varepsilon_{un} \leqslant 0.0035$ and $\varepsilon_{un} \geqslant 0.0035$. It should be noted that unloading can be initiated from the envelope curve, or from a reloading path as is the case in the tests of Specimens CI-RC and CII-RC in the present study. Only the plastic strain for unloading from the envelope curve can be directly related to the unloading strain, as shown in Fig. 4. This unloading strain is referred to as the envelope unloading strain $\varepsilon_{un,env}$. In Fig. 4, a linear relationship between the plastic strain and the envelope unloading strain is also observed for FRP-confined concrete, at least for $\varepsilon_{un,env} \geqslant 0.0035$. Fig. 4 shows that for the two series of specimens confined with one and two plies of CFRP respectively, the trend lines almost coincide. This appears to indicate that the plastic strain of FRP-confined concrete is independent of the amount of confinement. As both series of specimens had almost the same unconfined concrete strength, it is not clear whether the unconfined concrete strength has an effect on the plastic strain.

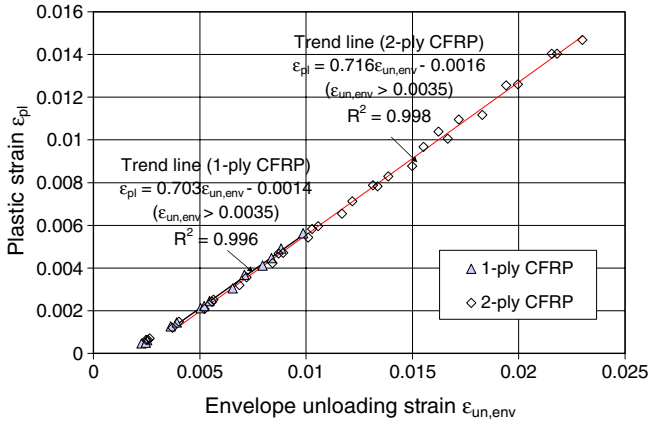

Fig. 4. Plastic strain versus envelope unloading strain.

4.3. Effect of loading history

Sinha et al. [4] suggested a uniqueness concept which means that the locus of common points, where the reloading path of an unloading/reloading cycle crosses the unloading path, can be considered as a stability limit. Stresses at or below this limit will lead to stress–strain responses following the same path without causing further permanent strains. According to this uniqueness concept, the effect of loading history is negligible in predicting the unloading and reloading paths of concrete. However, this uniqueness concept was not supported by subsequent tests by Karson and Jirsa [5]. This non-uniqueness concept has been verified by other studies on unconfined concrete and steel confined concrete (e.g. [10,12]).

The results of the present tests show that the uniqueness concept is also invalid for FRP-confined concrete. Figs. 2(c) and 3(c) show that when subjected to repeated cycles at each prescribed axial displacement level, the axial stress-axial strain response of a subsequent unloading/reloading cycle does not coincide with that of the previous cycle and instead shifts to the higher axial strain side. This shift of the unloading/reloading curve indicates a cumulative effect of the loading history on the permanent strain (plastic strain) and stress deterioration of FRP-confined concrete.

4.4. Ultimate condition

Extensive studies on FRP-confined concrete under monotonic compression have shown that eventual failure of FRP-confined concrete is by the rupture of the FRP jacket. The ultimate condition of the confined concrete, often characterized by the compressive strength and the ultimate axial strain, is thus intimately related to the ultimate tensile strain (or tensile strength) of the confining FRP in the hoop direction. Experimental results have shown that the material tensile strength of FRP for the hoop direction, defined as the tensile strength from coupon tensile tests, cannot be reached in FRP-confined concrete (e.g. [19,36,37]). A recent study by Lam and Teng [34] provided an in-depth examination of this important issue. In their study, the distribution of FRP hoop strains on confined cylinders of 152 mm in diameter was measured using a strain gauge layout as shown in Fig. 1. Lam and Teng [34] concluded that the smaller FRP strains on confined cylinders at hoop rupture than those obtained from coupon tensile tests are due to at least three causes: (a) the curvature of the FRP jacket; (b) the deformation non-uniformity of cracked concrete; and (c) the existence of an overlapping zone in which the measured hoop strains are much lower

than strains measured elsewhere. Lam and Teng [34] also noticed that the overlapping zone had little effect on the distribution of lateral confining pressure as the FRP jacket is thicker within this zone although the strains are smaller. Thus, they suggested using the average hoop strain from strain gauges outside the overlapping zone in calculating the lateral confining pressure.

The present study used the same hoop strain measurement scheme (Fig. 1) to study the ultimate condition of FRP-confined concrete under cyclic compression. All FRP-confined specimens tested in the present study failed by the rupture of the FRP jacket and the hoop rupture strains were smaller than the FRP material tensile strain. The distributions of FRP hoop strains at the last unloading/reloading cycle are shown in Fig. 5, and those at ultimate failure are shown in Fig. 6.

It is interesting to note that unloading/reloading cycles postponed the occurrence of hoop rupture failure. Table 1 shows that the FRP hoop rupture strains of cyclically loaded specimens are on average about 15% higher than those of the monotonically loaded specimens, in terms of both the maximum value around the circumference and the average value outside the overlapping zone. In this comparison, Specimen CI-SCI (cyclically loaded) was excluded, because one hoop strain gauge was damaged during loading. The higher FRP hoop rupture strains for cyclically loaded specimens have also been observed by Theodoros [29], although only average hoop strains were reported by him.

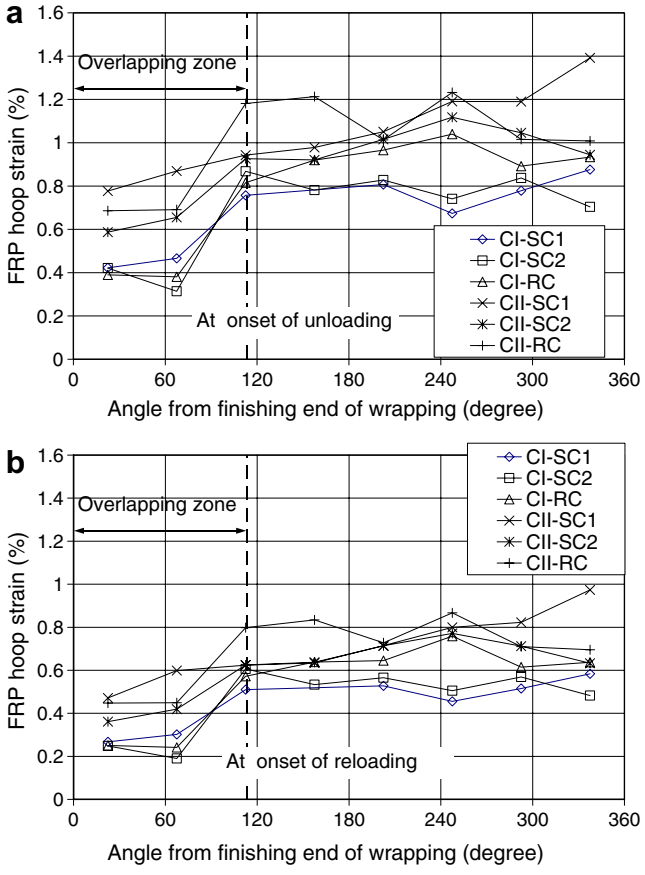

Fig. 5. Distributions of FRP hoop strains in the last unloading/reloading cycle. (a) At the onset of unloading and (b) at the onset of reloading.

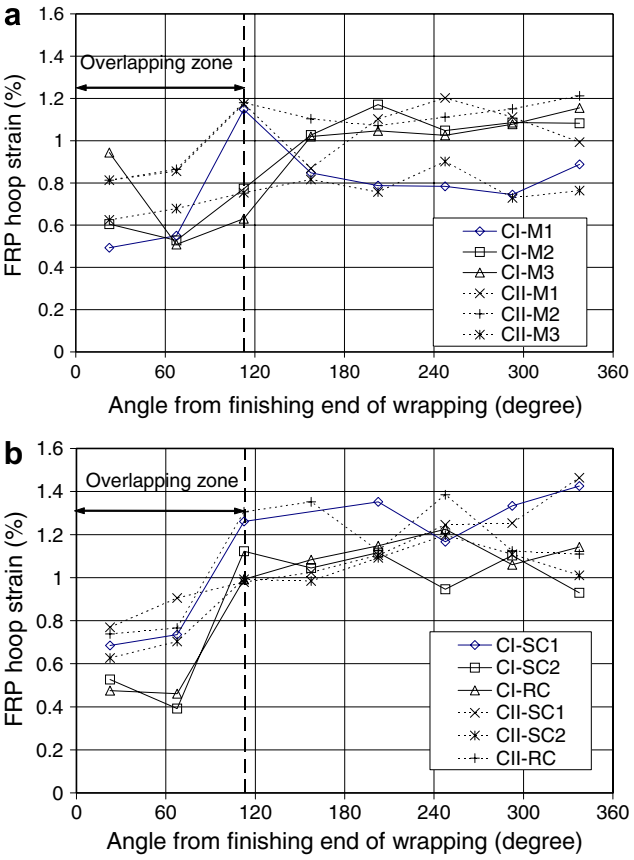

Fig. 6. Distributions of FRP hoop strains at failure. (a) Specimens under monotonic compression and (b) specimens under cyclic compression.

A comparison of specimens within the same series also indicates that apart from the FRP hoop rupture strain, the compressive strength and ultimate axial strain of FRP-confined concrete are also higher when loading is cyclically applied.

5. Comparison with existing stress–strain models

In this section, the present experimental results are compared first with a monotonic axial stress-axial strain model for FRP-confined concrete and then with a cyclic axial stress-axial strain model. For brevity, the term "stress–strain" is used to mean "axial stress-axial strain" in the following discussion.

5.1. Lam and Teng's model for monotonic stress–strain responses

The test results presented in the above section show that the cyclic stress–strain curve of FRP-confined concrete has an envelope curve which coincides with the monotonic curve. This observation suggests that a stress–strain model

for FRP-confined concrete developed based on monotonic tests can be used to predict the envelope curve of cyclic stress–strain responses. Of the existing models, a simple (i.e. design-oriented) but accurate model is that developed by Lam and Teng [24] based on a large test database assembled from the literature [38]. This model has several advantages over other design-oriented models for FRP-confined concrete in terms of accuracy and simplicity. In this model, the stress–strain curve of FRP-confined concrete is represented by a parabola as the first portion plus a straight line as the second portion, with a smooth transition between the two portions. The compressive strength and ultimate axial strain of FRP-confined concrete are predicted using the actual FRP hoop rupture strain. Details of this model can be found in Ref. [24].

Close agreement between the test results and the predictions by Lam and Teng's model [24] is seen in Figs. 7 and 8 for the stress–strain curves of monotonically loaded specimens and the envelope curves of cyclically loaded specimens respectively. Further comparisons between the tests and the predictions by Lam and Teng's model [24] for the compressive strength and the ultimate axial strain of FRP-confined concrete subject to cyclical loading are shown in Fig. 9(a) and (b). These comparisons show that although the FRP hoop rupture strains of cyclically loaded specimens are higher than those of monotonically loaded

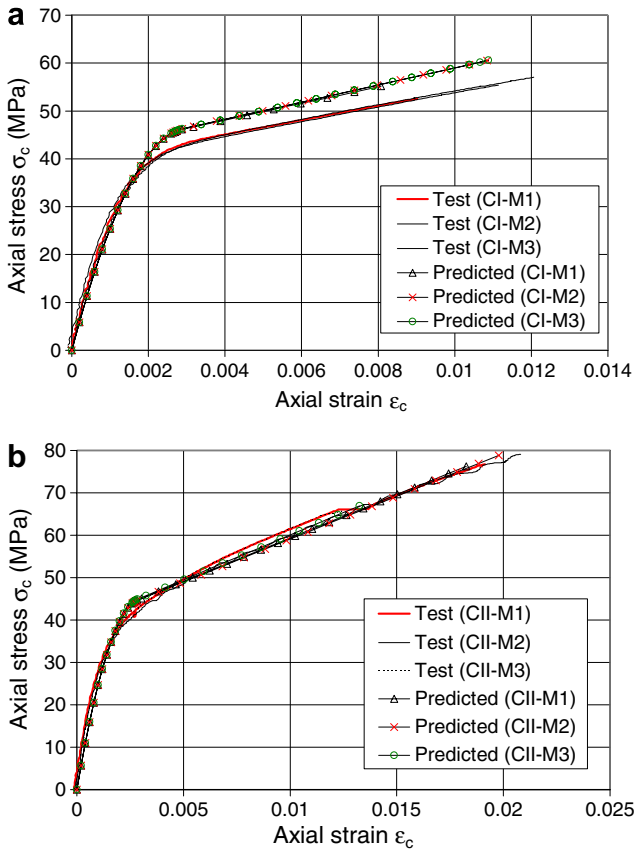

Fig. 7. Prediction of stress–strain curves of specimens under monotonic compression (a) Series I specimens and (b) Series II specimens.

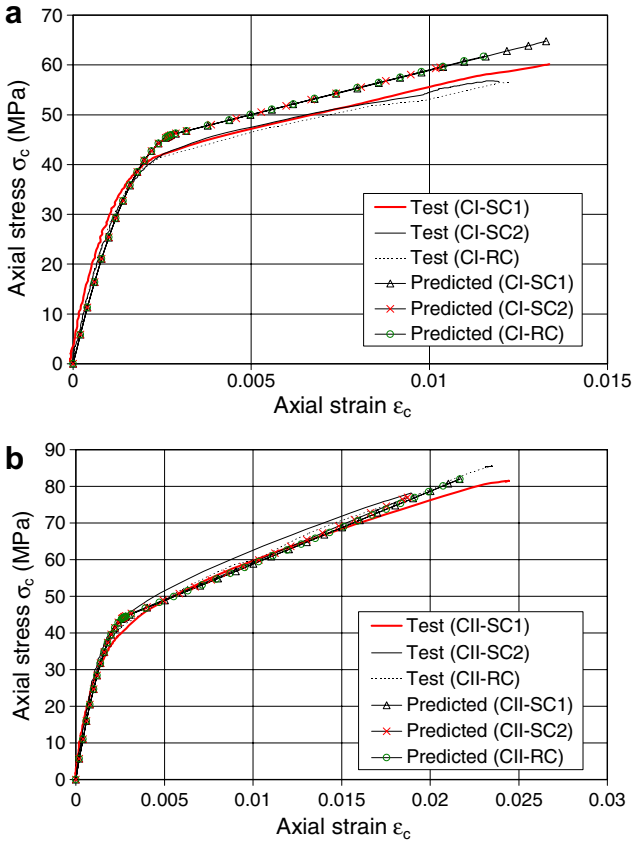

Fig. 8. Prediction of envelope curves of specimens under cyclic compression. (a) Series I specimens and (b) series II specimens.

specimens, the ultimate condition can still be closely predicted by Lam and Teng's model, provided that the actual hoop rupture strains are used. However, if FRP hoop rupture strains obtained from monotonic tests are used, Lam and Teng's model [24] leads to conservative predictions.

5.2. Shao's model for unloading and reloading paths

Shao [33] proposed a model for predicting the unloading/reloading hysteresis loops of FRP-confined concrete under cyclic compression. Details of this model are also available in Ref. [39]. In this model, the stress–strain model for monotonic behavior proposed by Samaan et al. [14] is used to predict the envelope curve. For unloading from the envelope curve, the stress–strain path is given by

$$\sigma_c = \frac{(1-x)^2}{(1+2x)^2}\sigma_{un,env} \quad (1)$$

where $\sigma_{un,env}$ is the stress at the envelope unloading strain, and x is defined as

$$x = \frac{\varepsilon_c - \varepsilon_{un,env}}{\varepsilon_{pl} - \varepsilon_{un,env}} \quad (2)$$

The plastic strain ε_{pl} is given by

$$\varepsilon_{pl} = \varepsilon_{un,env} - \frac{\sigma_{un,env}}{E_{sec\,u}} \quad (3)$$

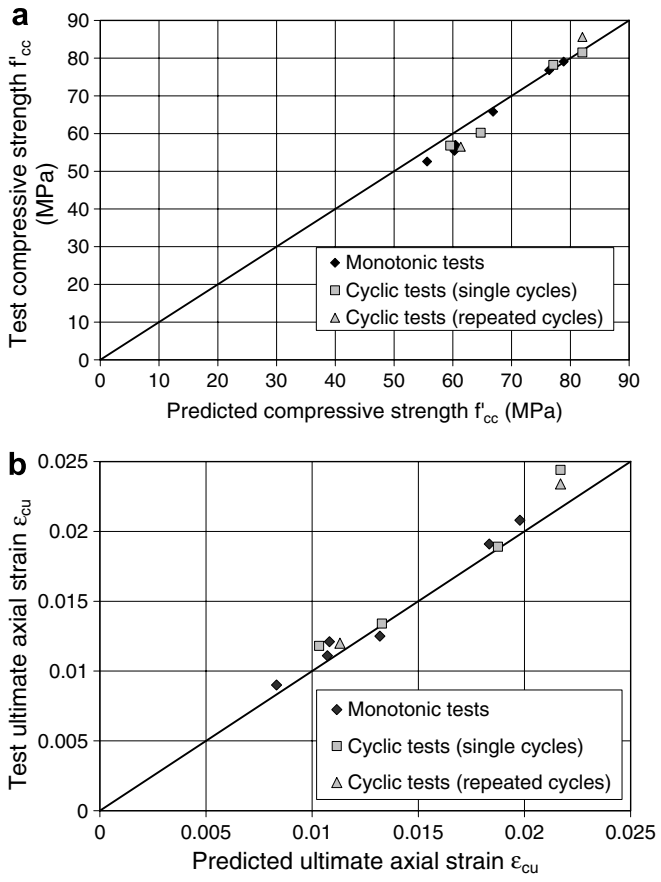

Fig. 9. Prediction of compressive strength and ultimate axial strain of FRP-confined concrete under monotonic and cyclic loading. (a) Compressive strength and (b) ultimate axial strain.

where $E_{\sec u}$ is the unloading modulus defined as

$$E_{\sec u} = \frac{\sigma_{\mathrm{un,env}}}{\varepsilon_{\mathrm{un,env}} - \varepsilon_{\mathrm{pl}}} \tag{4}$$

The following equation was proposed to evaluate the unloading modulus:

$$\frac{E_{\sec u}}{E_{\mathrm{c}}} = \begin{cases} 1, & 0 \leqslant \sigma_{\mathrm{un,env}}/f'_{\mathrm{co}} < 1 \\ -0.44\sigma_{\mathrm{un,env}}/f'_{\mathrm{co}} + 1.44, & 1 \leqslant \sigma_{\mathrm{un,env}}/f'_{\mathrm{co}} < 2.5 \\ 0.34, & \sigma_{\mathrm{un,env}}/f'_{\mathrm{co}} \geqslant 2.5 \end{cases} \tag{5}$$

where the elastic modulus of unconfined concrete $E_{\mathrm{c}} = 3950\sqrt{f'_{\mathrm{co}}}$ (MPa), as suggested by Samaan et al. [14]. Shao [33] suggested that for unloading from an arbitrary point, the stress–strain path should be predicted using Eqs. (1) and (2) with $\varepsilon_{\mathrm{un,env}}$ and $\sigma_{\mathrm{un,env}}$ replaced by $\varepsilon_{\mathrm{un}}$ and σ_{un}, the strain and stress at the unloading point respectively, while the plastic strain $\varepsilon_{\mathrm{pl}}$ remains the same as that determined from the envelope unloading strain $\varepsilon_{\mathrm{un,env}}$ using Eqs. (3)–(5).

Shao [33] proposed straight lines to represent reloading paths, as has been done by Mander et al. [8] and Bahn and Hsu [10] for unconfined or steel-confined concrete. To determine the reloading path, the new stress at the reference strain (the envelope unloading strain) σ_{new} on a reloading path is a key value, which is determined by

$$\sigma_{\mathrm{new}} = 0.9\sigma_{\mathrm{un,env}} \tag{6}$$

Shao [33] developed a number of rules for determining the stress–strain path, depending on the starting point of reloading. For reloading from a point with the stress being between zero and σ_{new}, which is the case for the present specimens, the reloading stress–strain path follows a straight line from the starting point of reloading to the reference strain point ($\varepsilon_{\mathrm{un,env}}, \sigma_{\mathrm{new}}$), and then follows anther straight line with the slope being that of a straight line connecting the plastic strain point to the reference strain point.

It should be noted that Shao's model makes use of the uniqueness concept. Consequently, the plastic strain and the new stress at the reference strain determined from the initial unloading/reloading cycle from the envelope curve are used for predicting the unloading and reloading paths of the subsequent cycles within the envelope curve. However, this uniqueness concept is not supported by the test results of the present study for FRP-confined concrete under cyclic compression. Thus, Shao's model is unable to predict the cumulative effect of loading history on the permanent strain and stress deterioration of FRP-confined concrete, as experienced by specimens CI-RC and CII-RC in the present study.

In Fig. 10, experimental plastic strains obtained in the present study are compared with the predictions by Eqs. (3)–(5) in Shao's model [33]. In Fig. 11, the experimental stress–strain curves of specimens CI-SC2 and CII-SC2 are compared with the unloading and reloading paths predicted using Shao' model. Envelope curves predicted using Samaan et al.'s model [14] and the actual FRP hoop rupture strains are also shown in this figure. In predicting the unloading paths, the experimental values of the unloading strain $\varepsilon_{\mathrm{un}}$, unloading stress σ_{un}, and plastic strain $\varepsilon_{\mathrm{pl}}$ were used. The use of the experimental plastic strains instead of the predictions of Eqs. (3)–(5) is because these equations overestimate the plastic strains of the present specimens considerably. In predicting the reloading paths,

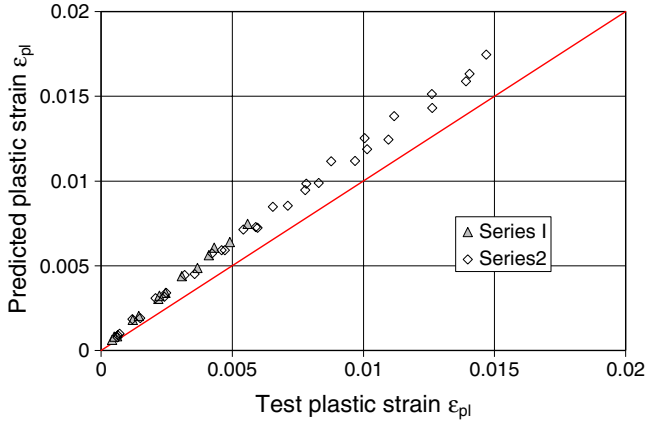

Fig. 10. Prediction of plastic strains using Shao's model.

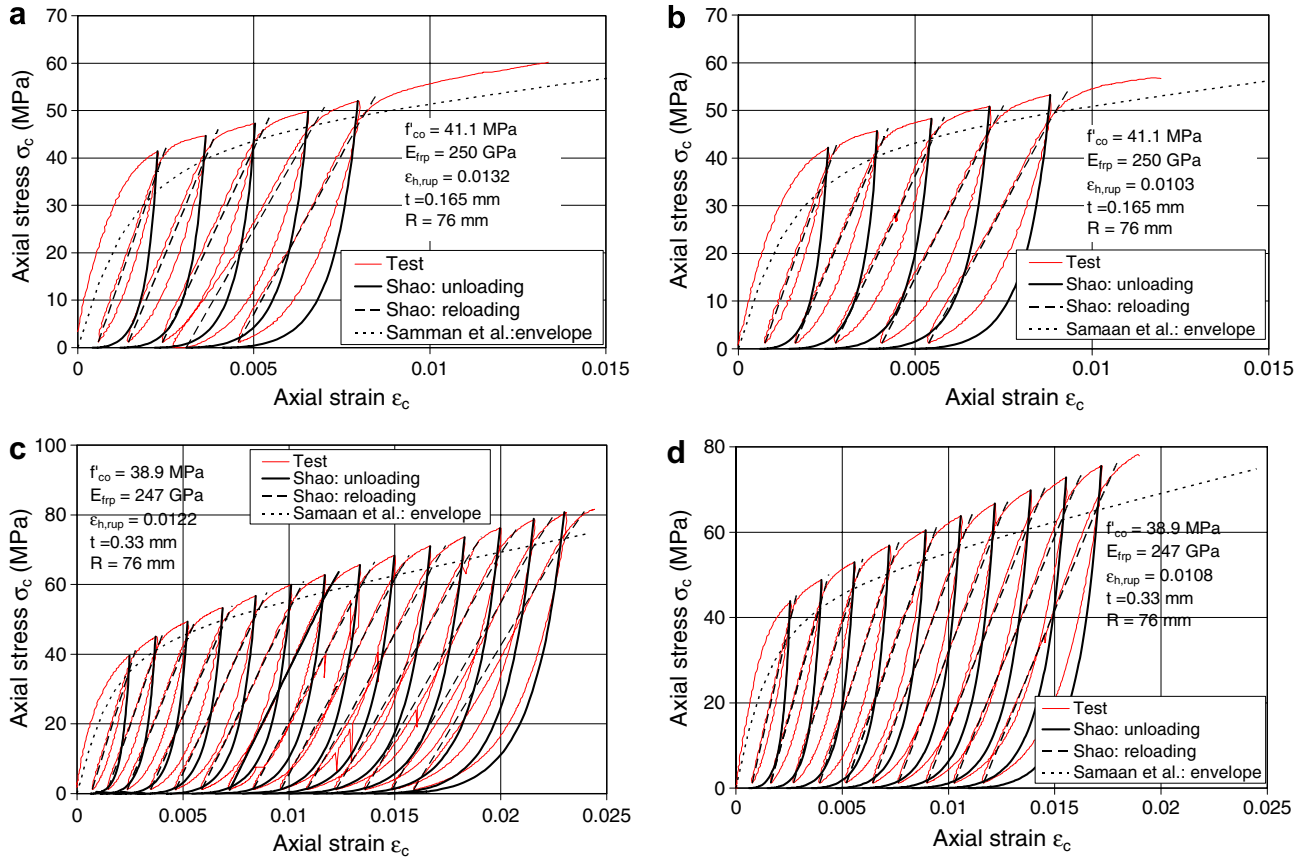

Fig. 11. Prediction of unloading and reloading paths using Shao's model. (a) Specimen CI-SC1, (b) specimen CI-SC2, (c) specimen CII-SC1, and (d) specimen CII-SC2.

experimental values of the stress and strain at the starting point of reloading, as well as the envelope unloading strain $\varepsilon_{un,env}$ and stress $\sigma_{un,env}$ were used, while the new stress at the reference strain point σ_{new} was found using Eq. (6). In Eq. (6), a factor of 0.9 is very close to the average value of 0.917 found from the present tests. According to Shao [33], the termination point of a reloading curve needs to be determined using Samaan et al.'s model [14], but in Fig. 4, these curves are terminated at approximately the experimental envelope curve instead of that given by Samaan et al.'s model [14] as the latter does not match the present test envelope curves well.

Fig. 10 shows that the experimental plastic strains are overestimated by Shao's model [33]. Fig. 11 shows that for the four specimens subjected to single unloading/reloading cycles at prescribed displacements, the predicted reloading paths match the test results reasonably well, but the predicted unloading paths do not. The two specimens subjected to repeated cycles at prescribed displacements are not used for comparison because Shao's model [33] does not cover this type of unloading/reloading cycles.

6. Conclusions

This paper has been concerned with the behavior and modeling of FRP-confined concrete under cyclic compression. Results from monotonic and cyclic compression tests on CFRP-confined concrete cylinders have been presented and discussed. The test results have also been compared with a monotonic stress–strain model and a cyclic stress–strain model for FRP-confined concrete. The following conclusions may be drawn from the present study:

1. Unloading/reloading cycles have little effect on the envelope curve of stress–strain responses of FRP-confined concrete, except for a small enhancement of the FRP hoop rupture strain.
2. For the same concrete strength, the plastic strain of FRP-confined concrete is linearly related to the envelope unloading strain, but is independent of the amount of FRP-confinement.
3. Repeated unloading/reloading cycles have a cumulative effect on the permanent strain and stress deterioration, so the uniqueness concept of cyclic stress–strain responses is invalid.
4. The envelope curve, compressive strength and ultimate axial strain of FRP-confined concrete can be accurately predicted using Lam and Teng's monotonic stress–strain model [24] for FRP-confined concrete, provided that the enhanced FRP hoop rupture strain is used.

5. The recent model proposed by Shao [33] is the only model available for predicting the stress–strain response of FRP-confined concrete under cyclic axial compression. Comparisons between the present test results and the predictions of this model indicated that this model predicts reloading paths reasonably closely but does not predict the unloading paths well. Another weakness of the model is that it makes use of the uniqueness assumption, which renders the model incapable of predicting the cumulative effect of loading history on the permanent strain and stress deterioration of concrete.

It should be noted the above conclusions have been reached on the basis of tests conducted on small-scale specimens (i.e. standard cylinders). Size effects may exist and such effects should be examined using full-scale specimens in the future.

Acknowledgements

The authors are grateful for the financial support received from the Research Grants Council of the Hong Kong SAR (Project No: Poly U 5059/02E) and The Hong Kong Polytechnic University (Project Codes: A232 and BBZH).

References

[1] Teng JG, Chen JF, Smith ST, Lam L. FRP-strengthened RC structures. John Wiley and Sons; 2002.
[2] Teng JG, Chen JF, Smith ST, Lam L. Behavior and strength of FRP-strengthened RC structures: a state-of-the-art review. ICE Proc: Struct Build 2003;156(1):51–62.
[3] Xiao Y. Applications of FRP composites in concrete column. Adv Struct Eng 2004;7(4):335–43.
[4] Sinha BP, Gerstle KH, Tulin LG. Stress–strain relations for concrete under cyclic loading. ACI J 1964;61(2):195–211.
[5] Karsan ID, Jirsa JO. Behavior of concrete under compressive loadings. J Struct Eng Div, ASCE 1969;95(ST12):2543–63.
[6] Buyukozturk O, Tseng TM. Concrete in biaxial cyclic compression. J Struct Eng, ASCE 1984;110(3):461–76.
[7] Shah SP, Fafitis A, Arnold R. Cyclic loading of spirally reinforced concrete. J Struct Eng, ASCE 1983;109(7):1695–710.
[8] Mander JB, Priestley MJN, Park R. Theoretical stress–strain model for confined concrete. J Struct Eng, ASCE 1988;114(8):1804–26.
[9] Maritinez-Rueda JE, Elnashai AS. Confined concrete model under cyclic load. Mater Struct 1997;30(April):139–47.
[10] Bahn BY, Hsu CTT. Stress–strain behavior of concrete under cyclic loading. ACI Mater J 1998;95(2):178–92.
[11] La Mendola L, Papia M. General stress–strain model for concrete or masonry response under uniaxial cyclic compression. Struct Eng Mechan 2002;14(4):435–54.
[12] Sakai J, Kawashima K. Unloading and reloading stress–strain model for confined concrete. J Struct Eng, ASCE 2006;132(1):112–22.
[13] Karbhari VM, Gao Y. Composite jacketed concrete under uniaxial compression-verification of simple design equations. J Mater Civil Eng ASCE 1997;9(4):185–93.
[14] Samaan M, Mirmiran A, Shahawy M. Model of concrete confined by fiber composite. J Struct Eng, ASCE 1998;124(9):1025–31.
[15] Miyauchi K, Inoue S, Kuroda T, Kobayashi A. Strengthening effects of concrete columns with carbon fiber sheet. Trans Jpn Conc Inst 1999;21:143–50.
[16] Saafi M, Toutanji HA, Li Z. Behavior of concrete columns confined with fiber reinforced polymer tubes. ACI Mater J 1999;96(4):500–9.
[17] Spoelstra MR, Monti G. FRP-confined concrete model. J Compos Const, ASCE 1999;3(3):143–50.
[18] Toutanji HA. Stress–strain characteristics of concrete columns externally confined with advanced fiber composite sheets. ACI Mater J 1999;96(3):397–404.
[19] Xiao Y, Wu H. Compressive behavior of concrete confined by carbon fiber composite jackets. J Mater Civil Eng, ASCE 2000;12(2):139–46.
[20] Xiao Y, Wu H. Compressive behavior of concrete confined by various types of FRP composite jackets. J Reinf Plast Compos 2003;22(13):1187–202.
[21] Fam AZ, Rizkalla SH. Confinement model for axially loaded concrete confined by circular fiber reinforced polymer tubes. ACI Struct J 2001;98(4):451–61.
[22] Teng JG, Lam L. Compressive behavior of carbon fiber reinforced polymer-confined concrete in elliptical columns. J Struct Eng, ASCE 2002;128(12):1535–43.
[23] Lam L, Teng JG. Strength models for fiber reinforced plastic-confined concrete. J Struct Eng, ASCE 2002;128(5):612–23.
[24] Lam L, Teng JG. Design-oriented stress–strain model for FRP-confined concrete. Const Build Mater 2003;17(6–7):471–89.
[25] Lam L, Teng JG. Design-oriented stress–strain model for FRP-confined concrete in rectangular columns. J Reinf Plast Compos 2003;22(13):1149–86.
[26] Mirmiran A, Shahawy M. Behavior of concrete columns confined by fiber composites. J Struct Eng, ASCE 1997;123(5):583–90.
[27] Rodrigues CC, Silva MG. Experimental investigation of CFRP reinforced concrete columns under uniaxial cyclic compression. Proceedings, fifth international conference on fibre-reinforced plastics for reinforced concrete structures. London, UK: Thomas Telford; 2001. p. 783–92.
[28] Rodrigues CC, Silva MG. The behavior of GFRP reinforced concrete columns under monotonic and cyclic axial compression. Composites in constructions, proceedings of the international conference. Lisse, The Netherlands: A.A. Balkema Publishers; 2001. p. 245–50.
[29] Theodoros R. Experimental investigation of concrete cylinders confined by carbon FRP sheets, under monotonic and cyclic axial compression load. Research Report. Publication 01: 2, Division of Building Technology, Chalmers University of Technology, 2001.
[30] Ilki A, Kumbasar N. Behavior of damaged and undamaged concrete strengthened by carbon fiber composite sheets. Struct Eng Mechan 2002;13(1):75–90.
[31] Ilki A, Kumbasar N. Compressive behavior of carbon fiber composite jacketed concrete with circular and non-circular cross sections. J Earthquake Eng 2003;7(3):381–406.
[32] Jin XN. Experimental study of the mechanical properties of axisymmetrically confined concrete. PhD Thesis, Harbin Institute of Technology, 2002 (in Chinese).
[33] Shao Y. Behavior of FRP-confined concrete beam-columns under cyclic loading. PhD Thesis, North Carolina State University, USA, 2003.
[34] Lam L, Teng JG. Ultimate condition of fiber reinforced polymer-confined concrete. J Compos Const, ASCE 2004;8(6):539–48.
[35] ASTM D3039/D3039M–95. Standard test method for tensile properties of polymer matrix composite materials. Annual Book of ASTM Standards 1995; vol. 14.02.
[36] Shahawy M, Mirmiran A, Beitelman T. Test and modeling of carbon-wrapped concrete columns. Compos Part B: Eng 2000;31:471–80.
[37] Pessiki S, Harries KA, Kestner JT, Sause R, Ricles JM. Axial behavior of reinforced concrete columns confined with FRP jackets. J Compos Const, ASCE 2001;5(4):237–45.
[38] Teng JG, Lam L. Behavior and modeling of fiber reinforced polymer-confined concrete. J Struct Eng, ASCE 2004;130(11):1713–23.
[39] Shao Y, Aval S, Mirmiran A. Fiber-element model of cyclic analysis of concrete-filled fiber reinforced polymer tubes. J Struct Eng, ASCE 2005;131(2):292–303.